ECCOMAS Congress 2016
VII European Congress on Computational Methods in Applied Sciences and Engineering
M. Papadrakakis, V. Papadopoulos, G. Stefanou, V. Plevris (eds.)
Crete Island, Greece, 5–10 June 2016

FLEXURAL VIBRATION ANALYSIS OF GRAPHENE NANOPLATELETS REINFORCED NANOCOMPOSITE BEAMS

Jie Yang and Chuang Feng

School of Engineering, RMIT University
PO Box 71, Bundoora, VIC 3083, Australia
{j.yang, chuang.feng}@rmit.edu.au

Keywords: Flexural Vibration, Nanocomposites, Graphene Nanoplatelet, Timoshenko Beam Theory

Abstract. *Polymer nanocomposites with the addition of a small percentage of graphenes as reinforcement have demonstrated tremendous potential to serve as next generation functional or structural materials due to their combination of high specific surface area, strong nanofiller-matrix adhesion and the outstanding mechanical properties of the sp2 carbon bonding network in graphene. While the majority of the work on graphene based composites has been focused on quantifying their mechanical properties, the vibration characteristics of graphene composites has not yet been investigated. This paper presents an analytical study on the flexural vibration of polymer beams reinforced with uniformly distributed graphene nanoplatelets (GPL). Based on the assumption that each graphene nanoplatelet acts as an effective rectangular solid fiber, the Halpin-Tsai model for fiber-reinforced composites is modified to predict the Young's modulus of the GPL/epoxy nanocomposites. Governing equations of motion are derived within the framework of linear elastic strain-displacement relationship and Timoshenko beam theory to account for transverse shear strain. The influences of GPL weight fraction, beam slenderness ratio and boundary conditions on the natural frequencies and associated mode shapes are investigated in detail. It is found that adding a very small amount of GPLs into the polymer matrix can effectively lead to a remarkable increase in beam stiffness hence the natural frequencies of the nanocomposite beams, and that the rate of frequency change of the beam is independent of the slenderness ratio.*

1 INTRODUCTION

Compared to carbon nanotubes (CNTs), graphene and its derivatives have demonstrated favorable advantages when used as reinforcing fillers in composites. For example, the ultimate strength and Young's modulus of graphene and its derivatives can reach up to 1 TPa and 130 GPa, respectively [1]. A recent experimental study [2] showed that with the same weight fraction of additives, i.e. 0.1±0.002%, Young's modulus of graphene based epoxy nanocomposites was 31% greater than that of pristine epoxy while an increase of 3% was observed when CNT fillers are used. This remarkable reinforcing effect stems from graphene's excellent mechanical properties and very high specific surface areas [2-7]. In addition, graphene's derivatives, i.e. graphene nanoplatelets, are in abundance in nature. This significantly expedites the engineering applications of graphene based composites due to their superior mechanical properties but moderate cost [8].

Extensive theoretical and experimental research work has been done on the fabrication and characterization of mechanical properties of graphene based nanocomposites. Rafiee et al. [2] fabricated functionalized graphene sheet (FGS)/epoxy nanocomposite and found this composite offers significant improvements in mechanical properties compared to those of CNT reinforced epoxy composites. Lee et al. [9] successfully synthesized FGS/epoxy nanocomposite whose strength was increased by approximately 30-80% at a loading of 1.6 wt%. Martín-Gallego et al. [10] studied the reinforcement of graphene and observed the significant improvement in mechanical properties of FGS-epoxy composites. Graphene is usually present in the form of agglomerates due to van der Waals force and the dispersion state is crucial to the performance of the composites. Tang et al. [6] discussed the effect of graphene dispersion on the mechanical properties of graphene/epoxy nanocomposites. They found the nanocomposites with highly dispersed graphene exhibit higher strength and better fracture toughness. This significant enhancement was also observed in other previous studies [1, 5, 7]. Among the theoretical studies, Rahman and Haque [11] investigated the mechanical properties of graphene platelet (GPL)/epoxy nanocomposites by molecular mechanics (MM) and molecular dynamics simulations (MD). Significant improvement in Young's modulus and shear modulus of the composites was observed. Cho and co-workers [12] predicted the elastic constants of graphite using MM and determined the elastic constants of graphite/epoxy nanocomposites by using Mori–Tanaka micromechanical model. Xiang et al. [13] also developed a micromechanics model for graphene/polymer nanocomposite based on Mori–Tanaka method. Spanos et al. [14] used a micromechanical finite element approach to obtain the mechanical properties of the composites reinforced with uniformly distributed graphenes. They found that their mechanical properties depend on the dimensions and volume fraction of graphenes as well as on the stiffness of the interphase between the two constituents. Chandra et al. [15] presented a multiscale model for vibration frequency analysis of graphene/polymer composites and observed exceptional vibrational behaviour and large stiffness of graphene reinforced composites.

It should be pointed out that although there has been a fast growing interest in graphene based polymer composites, the majority of the previous work is primarily focused on the material fabrication and characterization. Studies on the structural behaviour are very limited in number. This paper presents an analytical study on the flexural vibration of polymer nanocomposite beam in which GPLs are uniformly dispersed in epoxy matrix. Theoretical formulations are established within the framework of Timoshenko beam theory and linear strain-displacement relationship. The modified Halpin-Tsai model is used to predict the Young's modulus of the GPL/epoxy nanocomposites. A detailed parametric study is

conducted to discuss the influences of GPL weight fraction, beam slenderness ratio and boundary conditions on the natural frequencies and associated mode shapes of the beam.

2 GOVERNING EQUATIONS

2.1 Equations of motion

Shown in figure 1 is a GPL/epoxy nanocomposite beam with length *l*, width *b* and thickness *h*, subjected to a distributed dynamic load *q*(*x*, *t*). According to Timoshenko beam theory, the bending moment *M* and shear force *Q* are given as

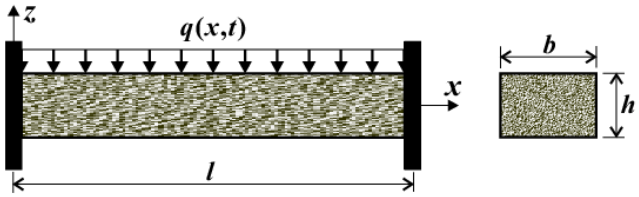

Figure 1: Schematic configuration of a GPL/epoxy nanocomposite beam.

$$M(x) = -E_c I \frac{\partial \varphi}{\partial x}, \quad Q(x) = \alpha A G_c (\frac{\partial w}{\partial x} - \varphi) \tag{1}$$

where shear correction factor α = 5/6, E_c and G_c are the effective Young's modulus and shear modulus of the beam, A and I are the area and second moment of the cross-section, and φ represents the cross-sectional rotation, respectively. The governing equations of the beam can be derived as

$$E_C I \frac{\partial^2 \varphi}{\partial x^2} - \alpha A G \varphi + \alpha A G \frac{\partial w}{\partial x} + \rho I \frac{\partial^3 w}{\partial x \partial t^2} = 0 \tag{2}$$

$$\alpha A G \frac{\partial^2 w}{\partial x^2} - \alpha A G \frac{\partial \varphi}{\partial x} + bq(x,t) = \rho A \frac{\partial^2 w}{\partial t^2} \tag{3}$$

where ρ is the mass density of the beam. Combining equations (2) and (3) and eliminating φ leads to the equation of motion

$$E_c I \frac{\partial^4 w}{\partial x^4} - \rho I \left(1 + \frac{E_c}{G_c \alpha}\right) \frac{\partial^4 w}{\partial x^2 \partial t^2} + \rho A \frac{\partial^2 w}{\partial t^2} = q_0 cos(\omega_e t) \tag{4}$$

where $q = q_0 \cos(\omega_e t)$ with q_0 and ω_e being the amplitude and radian frequency of the transverse load. Introducing the following dimensionless quantities

$$X = \frac{x}{l}, \; W = \frac{w}{h}, \; \eta = \frac{l}{h}, \; \tau = \frac{t}{l}\sqrt{\frac{E_c}{\rho_c}}, \; Q_0 = \frac{12 q_0 \eta^4}{E_c} \tag{5}$$

equation (4) can be cast into the following dimensionless form

$$\frac{\partial^4 W}{\partial X^4} - [1 + 2(1+\nu)\frac{1}{\alpha}] \frac{\partial^4 W}{\partial X^2 \partial \tau^2} + 12\eta^2 \frac{\partial^2 W}{\partial \tau^2} = Q_0 \cos(\omega \tau) \tag{6}$$

where $\omega = \omega_e l \sqrt{\rho_c / E_c}$ is the dimensionless excitation frequency.

2.2 Halpin-Tsai model for GPL/polymer nanocomposites

Assuming that GPLs serve as effective rectangular solid fillers uniformly dispersed in the polymer matrix, the effective Young's modulus of the nanocomposite can be approximated by employing modified Halpin-Tsai micromechanics model as [2, 16-18]

$$E_{\mathrm{C}}=\frac{3}{8}\frac{1-\xi\eta_{\mathrm{L}}V_{\mathrm{eff,GPL}}}{1-\eta_{\mathrm{L}}V_{\mathrm{eff,GPL}}}\times E_{\mathrm{M}}+\frac{5}{8}\frac{1-\xi\eta_{\mathrm{W}}V_{\mathrm{eff,GPL}}}{1-\eta_{\mathrm{W}}V_{\mathrm{eff,GPL}}}\times E_{\mathrm{M}} \tag{7}$$

where E_{M} is Young's modulus of the matrix, $V_{\mathrm{eff,GPL}}$ is GPLs' volume fraction, $\xi=(l_{\mathrm{GPL}}+w_{\mathrm{GPL}})/h_{\mathrm{GPL}}$, $\eta_{\mathrm{L}}=\frac{(E_{\mathrm{eff,GPL}}/E_{\mathrm{M}})-1}{(E_{\mathrm{eff,GPL}}/E_{\mathrm{M}})+\xi}$ and $\eta_{\mathrm{W}}=\frac{(E_{\mathrm{eff,GPL}}/E_{\mathrm{M}})-1}{(E_{\mathrm{eff,GPL}}/E_{\mathrm{M}})+2}$ in which l_{GPL}, w_{GPL}, h_{GPL} and E_{GPL} are the length, width, thickness, and Young's modulus of GPLs, respectively. Given the mass density of GPLs ρ_{GPL} and that of polymer matrix ρ_{M}, GPLs' volume fraction in the nanocomposite can be approximated as

$$V_{\mathrm{GPL}}=\frac{f_{\mathrm{GPL}}}{f_{\mathrm{GPL}}+\left(\rho_{\mathrm{GPL}}/\rho_{\mathrm{M}}\right)\left(1-f_{\mathrm{GPL}}\right)} \tag{8}$$

where f_{GPL} is the weight fraction of the GPLs in the composite.

Equation (7) was used to estimate the effective Young's modulus of GPL/polymer nanocomposites and has been experimentally validated by Rafiee et al. [2]. It is assumed that Poison's ratio is v = 0.4 due to the fact that the mechanical behavior of the nanocomposite is weakly dependent on Poisson's ratio. This is verified in our numerical simulations which indicate that Poison ratio has a very limited effect on the vibration of the beam.

3 SOLUTION

3.1 Free vibration

For free vibration, the governing equation is reduced to

$$\frac{\partial^4 W}{\partial X^4}-[1+2(1+\nu)\frac{1}{\alpha}]\frac{\partial^4 W}{\partial X^2\partial\tau^2}+12\eta^2\frac{\partial^2 W}{\partial\tau^2}=0 \tag{9}$$

For harmonic vibration, the transverse displacement can be written as

$$W(X,\tau)=\emptyset(X)e^{i\omega_l\tau} \tag{10}$$

where $\omega_l=\Omega l\sqrt{\rho_c/E_c}$ is the dimensionless linear natural frequency with Ω being the natural frequency of the beam. Substituting equation (10) into (9), the solution to the resulting differential equation is

$$\emptyset(X)=C_1 sinh\,(\lambda_1 X)+C_2 cosh(\lambda_1 X)+C_3\,sin(\lambda_2 X)+C_4 cos(\lambda_2 X) \tag{11}$$

where

$$\lambda_{1,2}^2=\frac{-\left[1+2\left(1+\nu\right)\frac{1}{\alpha}\right]\omega_l^2\pm\sqrt{\left[1+2\left(1+\nu\right)\frac{1}{\alpha}\right]^2\omega_l^4+48\eta^2\omega_l^2}}{2} \tag{12}$$

and C_1 to C_4 are unknown constants to be determined by associated boundary conditions.

In this paper, clamped-clamped (C-C), clamped-hinged (C-H) and hinged-hinged (H-H) beams are considered, with the following boundary conditions

a) C-C beam: $\emptyset(0)=\emptyset(1)=\frac{d\emptyset(0)}{dx}=\frac{d\emptyset(1)}{dx}=0$;
b) C-H beam: $\emptyset(0)=\emptyset(1)=\frac{d\emptyset(0)}{dx}=M(1)=0$;
c) H-H beam: $\emptyset(0)=\emptyset(1)=M(0)=M(1)=0$.

The boundary conditions for each case will result in an algebraic equation, i.e. $[H(\omega_l)]\{\chi\}=\{0\}$. $H(\omega_l)$ is a matrix dependent on ω_l while χ is a vector consisting of the four

unknown coefficients. The non-trivial solution of χ requires the determinant of the $H(\omega_l)$ be zero, from which the natural frequencies and the associated mode shapes can be obtained.

3.2 Forced harmonic vibration

For forced harmonic vibration, the transverse displacement is approximated as

$$W(X,\tau) = S(\tau)\emptyset(X) \tag{13}$$

where $\emptyset(X)$ is the mode shape obtained from free vibration analysis and $S(\tau)$ denote the vibration characteristics to be determined. Substituting equation (13) into equation (6) and applying Galerkin method, the governing equation becomes

$$\ddot{S}(\tau)+\gamma S = Q_E\cos(\omega\tau) \tag{14}$$

where

$$\begin{cases} \gamma = -\dfrac{1}{\gamma_o}\displaystyle\int_0^1\left(\phi\frac{d^4\phi}{dX^4}\right)dX, \quad Q_E = \dfrac{Q_0}{\gamma_o}\displaystyle\int_0^1\phi dX \\ \gamma_o = \displaystyle\int_0^1\left[12\eta^2\phi^2 - \left(1+\frac{2(1+\nu)}{\alpha}\right)\phi\frac{d^2\phi}{dX^2}\right]dX \end{cases} \tag{15}$$

The dynamic response of the beam under transverse loading is obtained as

$$S(\tau) = \left(S_0 - \frac{Q_0}{\gamma-\omega^2}\right)\cos(\omega_l\tau) + \frac{\dot{S}_0}{\omega_l}\sin(\omega_l\tau) + \frac{Q_0}{\gamma-\omega^2}\cos(\omega\tau) \tag{16}$$

4 RESULTS AND DISCUSSION

Table 1 compares our results with the previous data [19] for the natural frequency of a homogeneous beam whose Young's modulus, mass density and Poisson's ratio are E = 70 GPa, ν = 0.33 and ρ = 2780 kg/m^3, respectively. Excellent agreement is observed.

C-C		H-H	
Present	Ref [19]	Present	Ref [19]
5.5933	5.59	2.4674	2.47

Table 1: Comparison of linear natural frequency.

In what follows, the dimensions, mass density, Young's modulus and weight fraction of GPLs are l_{GPL} = 2.5 μm, w_{GPL} = 1.5 μm, t_{GPL} = 1.5 nm, ρ_{GPL} = 1.06 g/cm^3, E_{GPL} = 1.01 TPa, and f_{GPL} = 1.5%, respectively [2]. Young's modulus of the epoxy matrix is E_M = 3.0 GPa. Table 2 lists the first three dimensionless frequencies of the nanocomposite beams with different end supports. The associated mode shapes are displayed in figure 2. As expected, the frequencies are the highest for a C-C beam and the lowest for an H-H beam. The significant reinforcing effect of GPLs on the dynamic characteristics of the beam is clearly evidenced by over 60% increase in the natural frequencies as compared to those of pristine epoxy beams.

Mode	C-C		C-H		H-H	
	Pure epoxy	Composite	Pure epoxy	Composite	Pure epoxy	Composite
1	0.3090	0.5057	0.2031	0.3426	0.1151	0.2108
2	0.8715	1.4060	0.7000	1.1351	0.5445	0.8918
3	1.7247	2.7665	1.4822	2.3823	1.2571	2.0263

Table 2: Dimensionless natural frequency of composite beam.

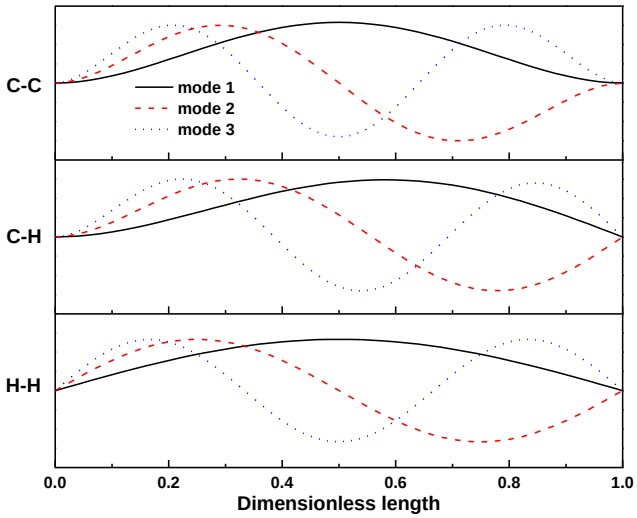

Figure 2: Mode shapes for nanocomposite beams with different boundary conditions.

The dimensionless fundamental frequency of a C-C beam versus slenderness ratio is shown in figure 3. It is easily understood that the frequency decreases as the slenderness ratio increases. At the same slenderness ratio, the natural frequency of the beam with GPL reinforcement is higher than that of the pure epoxy beam. This is due to the significantly increased effective Young's modulus of the beams when reinforced with GPLs, regardless of the end supports of the beams.

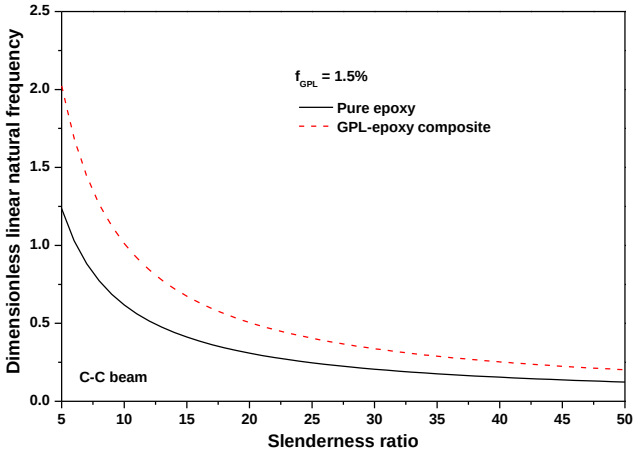

Figure 3: Variation of dimensionless fundamental frequency with beam slenderness ratio.

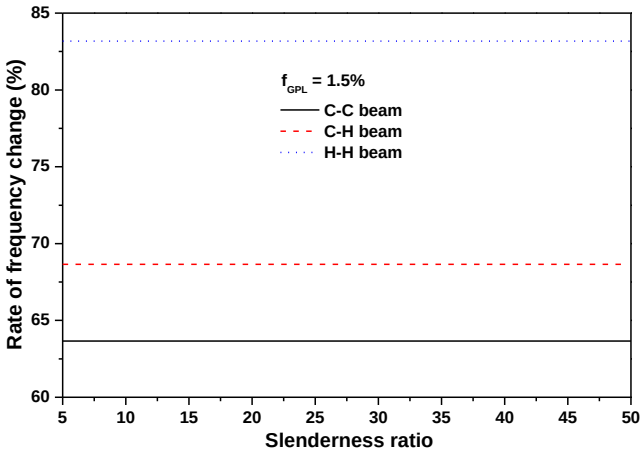

Figure 4: Effect of slenderness ratio on frequency change

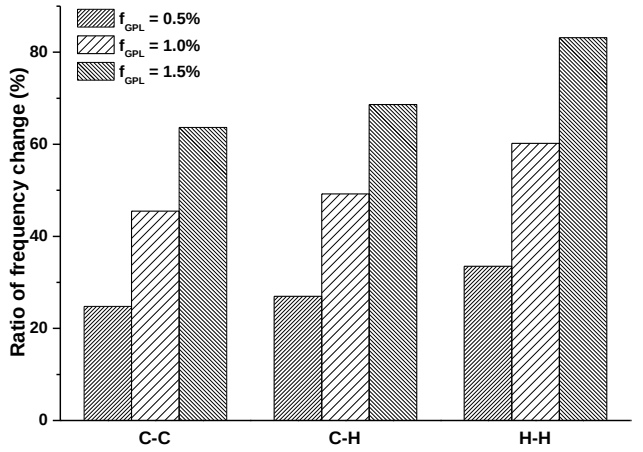

Figure 5: Effect of GPL weight fraction on frequency change.

Figure 4 presents the effect of slenderness ratio on the frequency change $(f_c–f_0)/f_0$, where f_c and f_0 denote the natural frequencies with and without GPLs. It is seen that the frequency gain is the highest for H-H beam (82.5%) whereas the lowest for C-C beam (63%). The rate of frequency change, however, is independent of the slenderness ratio for all beams. As revealed by figure 5, the frequency gain is almost doubled as the GPL weight fraction increases from 0.5% to 1.5%.

Figure 6 shows the dimensionless free vibration amplitudes of C-C, C-H and H-H beams under initial condition $W(0) = 0.1$ and $\dot{W}(0) = 0$. The vibration period, which is the lowest for the C-C beam among the three beams considered, becomes smaller when the beam is reinforced with GPLs. Figure 7 presents the dynamic responses of the same beams under a harmonic load $Q_E = 0.001$. As can be seen, the H-H beam has the highest vibration amplitude. Compared with the pure epoxy beam, the maximum vibration amplitude is considerably reduced with the addition of 1.5% w.t. GPLs into the epoxy matrix, confirming once again the remarkable reinforcing effect of GPLs on the dynamic performance of the beams. It should be also noted that this effect is most prominent in H-H beams. This is consistent with the observations obtained in natural frequencies.

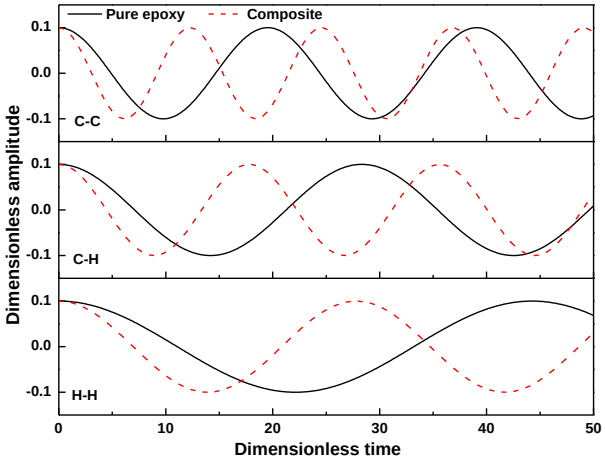

Figure 6: Dimensionless free vibration response of beams with different end supports.

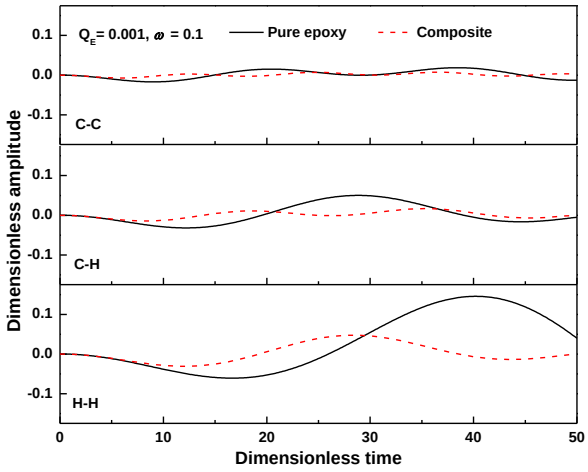

Figure 7: Dimensionless forced vibration response of beams with different end supports.

5 CONCLUSIONS

- Free and forced vibrations of GPL reinforced nanocomposite beam have been analytically investigated within the framework of Timoshenko beam theory.
- The addition of a very small amount of GPLs can significantly improve the free and forced vibration performance of the nanocomposite beams.
- The rate of frequency change increases at a higher GPL weight fraction but is independent of the slenderness ratio of the beam.
- Among the three boundary conditions considered, the reinforcing effect of GPLs is more significant for an H-H beam than the other two.

REFERENCES

[1] I. Zaman, T.T. Phan, H.-C. Kuan, Q. Meng, L.T.B. La, L. Luong, et al., Epoxy/graphene platelets nanocomposites with two levels of interface strength. *Polymer*, 52, 1603-1611, 2011.

[2] M.A. Rafiee, J. Rafiee, Z. Wang, H. Song, Z.Z. Yu, N. Koratkar, Enhanced mechanical properties of nanocomposites at low graphene content. ACS nano, 3, 3884-3890, 2009.

[3] M.M. Shokrieh, M. Esmkhani, Z. Shokrieh, Z. Zhao, Stiffness prediction of graphene nanoplatelet/epoxy nanocomposites by a combined molecular dynamics–micromechanics method. Computational Materials Science, 92, 444-450, 2014.

[4] T. Kuilla, S. Bhadra, D. Yao, N.H. Kim, S. Bose, J.H. Lee, Recent advances in graphene based polymer composites. Progress in polymer science, 35, 1350-1375, 2010.

[5] [5] X. Zhao, Q. Zhang, D. Chen, P. Lu, Enhanced mechanical properties of graphene-based poly (vinyl alcohol) composites. Macromolecules, 43, 2357-2363, 2010.

[6] L.C. Tang, Y.J. Wan, D. Yan, Y.B. Pei, L. Zhao, Y.B. Li, et al., The effect of graphene dispersion on the mechanical properties of graphene/epoxy composites. Carbon, 60, 16-27, 2013.

[7] S.K. Yadav, J.W. Cho, Functionalized graphene nanoplatelets for enhanced mechanical and thermal properties of polyurethane nanocomposites. Applied surface science, 266, 360-367, 2013.

[8] J.R. Potts, D.R. Dreyer, C.W. Bielawski, R.S. Ruoff, Graphene-based polymer nanocomposites. Polymer, 52, 5-25, 2011.

[9] J.K. Lee, S. Song, B. Kim, Functionalized graphene sheets- epoxy based nanocomposite for cryotank composite application. Polymer Composites, 33, 1263-1273, 2012.

[10] M. Martín-Gallego, R. Verdejo, M. Lopez-Manchado, M. Sangermano, Epoxy-graphene UV-cured nanocomposites. Polymer, 52, 4664-4669, 2011.

[11] R. Rahman, A. Haque, Molecular modeling of crosslinked graphene–epoxy nanocomposites for characterization of elastic constants and interfacial properties. Composites Part B: Engineering, 54, 353-364, 2013.

[12] J. Cho, J. Luo, I. Daniel, Mechanical characterization of graphite/epoxy nanocomposites by multi-scale analysis. Composites science and technology, 67, 2399-2407, 2007.

[13] X.Y. Ji, Y.P. Cao, X.Q. Feng, Micromechanics prediction of the effective elastic moduli of graphene sheet-reinforced polymer nanocomposites. Modelling and Simulation in Materials Science and Engineering, 18, 045005, 2010.

[14] K. Spanos, S. Georgantzinos, N. Anifantis, Mechanical properties of graphene nanocomposites: A multiscale finite element prediction. Composite Structures, 132, 536-544, 2015.

[15] Y. Chandra, R. Chowdhury, F. Scarpa, S. Adhikari, J. Sienz, C. Arnold, et al., Vibration frequency of graphene based composites: A multiscale approach. Materials Science and Engineering: B, 177, 303-310, 2012.

[16] P.K. Mallick, Fiber-reinforced composites: materials, manufacturing, and design. CRC press, 2007.

[17] E.T. Thostenson, T.W. Chou, On the elastic properties of carbon nanotube-based composites: modelling and characterization. Journal of Physics D: Applied Physics, 36, 573, 2003.

[18] J.C. Halpin, Effects of Environmental Factors on Composite Materials. DTIC Document, 1969.

[19] J. Yang, Y. Chen, Free vibration and buckling analyses of functionally graded beams with edge cracks. Composite Structures, 83, 48-60, 2008.